Impact of QuikSCAT Surface Marine Winds on Wave Hindcasting

V.J. Cardone, A. T. Cox, E. L. Harris, E. A. Orelup and M. J. Parsons
Oceanweather, Inc.
Cos Cob, CT
and
H. C. Graber
Rosenstiel School of Marine and Atmospheric Science
U. of Miami
Miami, Florida

1. INTRODUCTION

It is well known that the difficulty of specifying accurate marine surface wind fields has been a limiting factor in the refinement, evaluation and application of numerical wave models. There have been a few exceptions. For example, the SWADE IOP-1 hindcast (Cardone et al., 1995) demonstrated that given the unusually dense array of wind measurement platforms in the SWADE ocean region, it was possible to specify the time and space evolution of the marine surface layer wind field with no bias and very high accuracy and thereby allow very accurate deep water wave hindcasts of a stormy multi-week period off the U.S. mid-Atlantic coast. The same wind field analysis method applied in a data rich region to two very intense storms (Cardone et al., 1996) south of the Canadian Maritime Provinces allowed the resolution of subtle differences in model behavior between otherwise closely calibrated second and third generation models and revealed a failing common to all models tested in that the most extreme sea states (significant wave height greater than 12 m) were under-predicted. Similarly, detailed kinematic reconstructions of surface wind fields in some recent intense hurricanes from in-situ and aircraft data sources, including reduced flight level winds and GPS dropwindsonde wind measurements (Powell et al., 1998) have allowed specification of very accurate surface wind forcing and resulting wave hindcasts for the purposes of detailed engineering studies of offshore infrastructure response and damage and reassessment of metocean design criteria (e.g. Cardone et al., 2004; Puskar et al. 1994; Moon et al., 2003).

In general, however, wave hindcasts of continuous multi-decadal periods for purposes of climate assessment are typically driven by wind fields that possess known biases and poor resolution of the high-energy cores of tropical cyclones and intense extratropical cyclones. A notable exception in this regard was the 40-year North Atlantic AES40 hindcast (Swail and Cox, 2000), which included the expenditure of thousands of meteorologist labor-hours on kinematic reanalysis of surface marine wind fields through use of an interactive wind work workstation. It would be impractical to apply this approach to generate wind fields for larger basins or for a full global ocean hindcast.

The database of scatterometer marine surface winds provided by the SeaWinds instrument on the QuikSCAT (QS) satellite, launched in June 1999, has achieved a five-year continuous record. This record provides not only the opportunity to produce by direct assimilation of QS winds a very high quality multi-year global marine wind data set, but also a basis for the identification of the systematic component of errors that continue to characterize the marine wind fields of even the recent historical atmospheric "reanalysis" project datasets such as the 50-year NCEP/NCAR Reanalysis (NRA) and the ECMWF 40+ year (ERA40) projects. In this paper we affirm the intrinsic accuracy of QS winds over a wide dynamic range based both on published comparisons with measurements made by anemometers on buoys and research vessels, and new comparisons with winds measured by anemometers at "top of derrick" exposure on offshore platforms in the North Sea and Norwegian Sea. Next, we describe impacts of QS on hindcasting through direct assimilation of SeaWinds data as well as indirect impact by using SeaWinds based simple parametric statistical relationships to minimize systematic errors in the NRA winds.

2. FULL DYNAMIC RANGE EVALUATION OF SEAWINDS

2.1 Scatterometer Data

SeaWinds is the name of the Ku band scatterometer launched on QS on 19 June, 1999 following the early demise of the NSCAT Ku band scatterometer on ADEOS-1. Unlike earlier fan beam scatterometers such as the NSCAT and the ERS instruments, Sea Winds is the first scatterometer to scan conically with a dual-beam antenna such that it transmits and receives microwave radiation (13.4 GHz) at two incidence angles. At the satellite altitude of 803 km, the inner and outer beam widths yield a total swath width of 1800 km on the sea surface with no nadir gap, and this provides coverage of more than 95% of the globe every 24-hours. Only within the inner 1400 km of the swath, however, are their inner and outer beam overlapping measurements of backscatter cross-section, which yield four basic azimuth measurements from forward and backward looks (separated by a few minutes). The basic instantaneous fields of view on the sea surface are elliptical and approximately 25 km (azimuth) by 37 km (look or range direction), and in the process of geophysical wind retrieval anywhere between 10-25 individual footprints are used to produce a wind speed and direction at each cell of a 25 by 25 km grid laid out across the swath. Much has been written about the basis for retrieval of vector wind from four backscatter "looks" (e.g. Freilich, Long and Spencer, 1994) the calibration of the underlying geophysical model function (GMF) that relate backscatter and effective neutral 10-meter average surface wind (e.g. Wentz and Smith, 1999) and the various algorithms proposed to avert ambiguity in the retrieval of wind direction. In this study we utilize the result of the JPL QS science quality processed data, which is available in two versions that use the same GMF but differ in the ambiguity removal techniques. The so-called Level 2B (L2B) version uses the system applied to NSCAT while the so-called DIRTH (Direction Interval Retrieval Threshold, see Huddleston and Stiles, 2000) is claimed to provide a somewhat less noisy array of retrievals. We used DIRTH for our studies because small-scale variability is not a desirable trait for wind fields to be applied to force ocean response models. The Level 2B and DIRTH processing include the generation for each cell of a binary quality flag to indicate the possible contamination of the wind retrievals by rain, adjacent land and sea ice. We filtered all flagged data in the studies reported herein.

2.2 Surface Truth

Studies of the accuracy of QS winds against moored ocean data buoy (e.g. Ebuchi et al., 2002) and research vessel data (Bourassa et al., 2003) have well established the basic high level of skill in L2B and DIRTH wind speed and direction retrievals in the wind speed range up to about 20 m/s. For example, Ebuchi et al. report a mean QS-buoy difference in wind speed (expressed as effective neutral 1-hour averages at 10-

meter height) of 0.05 m/s and rms difference of 1.00 m/s in nearly 50,000 comparisons of QS winds and the global buoy dataset. However, there are only 14 comparisons with buoy wind speeds greater than 20 m/s in that dataset and they may be biased, and none greater than 24 m/s. Recent evaluations of the newer NWP reanalysis products suggest that at least in mid-latitude Northern Hemisphere regions such wind fields are already quite accurate and unbiased in the sub-20 m/s wind speed range. For the purposes of ocean response modeling to establish design data for example, it is the bias in the upper half of the naturally occurring dynamic range of 10-m hourly average wind speeds of 20 - 40 m/s that must be minimized. Therefore, we have focused on the exploration of the accuracy of QS wind retrievals in this range.

It is extremely difficult to obtain high quality in-situ wind data in high wind regimes. Winds measured by small-hulled or small-discus moored buoys with low mounted anemometers (< 5 meters) have been the predominant source of "surface truth" for validation of scatterometer winds and yet these measurements become increasingly biased negatively above wind speeds of about 20 m/s (e.g Taylor et al., 1999). Ordinary ship report winds are of poor quality in this range, and research vessels rarely sample this regime. Finally, marine wind fields produced by numerical weather prediction (NWP) centers, including even the products of the newer "reanalysis" projects, are notoriously biased low in severe storms (e.g. Swail and Cox, 2000).

In a previous pilot study (Cardone et al., 2000) that utilized a smaller sample of NSCAT data, it was shown that winds measured at the tops of drilling derricks at heights generally in the range 80 m up to 140 m at offshore platforms in the North Sea and Norwegian Sea provided perhaps a unique source of high-quality in-situ extreme surface wind measurements. After reduction to 10 m level and equivalent neutral conditions, the dataset collocated with NSCAT contained wind speeds up to 32 m/s. The validation clearly showed that while the NSCAT retrievals were sensitive to surface wind speed up to at least 32 m/s, the NSCAT 25-km winds appeared to underestimate surface wind speeds in the 25-35 m/s range by about 15%.

For this study we assembled a similar platform wind data set during the QS period utilizing the following six platforms: Draugen, Ekofisk, Gullfaks, Heidrun, Sleipner and K-13. The first five of these platforms are installed in water depth greater than 100 meters with calibrated instruments at the derrick-top exposure. The analysis presented in this paper is based on data assembled for the period July 1999 through December 2002. Figure 1 shows the locations of these platforms and their anemometer heights. Table 1 gives the platform data details. All wind data were obtained from the Norwegian Meteorological Institute (DNMI) from quality controlled archives, except for data from K-13, a platform located in Dutch waters, which was downloaded from the KNMI web site. Wind speeds are averaged typically over 10-minute or 20-minute intervals and recorded continuously, thereby allowing us to recover the one-hour average using averaged values from +/- 29 minutes from the top of the hour.

Typically, platform wind speeds are reduced from sensor height to 10 m level before recording and transmission, using constant reduction factors derived from the power law relationship. K-13 is the only platform in this dataset that uses an explicit profile for this purpose. The constant reduction factors vary from platform to platform and since they are known (see Table 1) they were applied in this study to first recover the actual measured average wind speed at sensor height before proceeding with the analysis.

One drawback of the platform data is that the very high anemometer heights amplify the differences in reduced 10-m wind speeds between seemingly similar profile laws. In Cardone et al. (2000) the boundary layer models of Cardone (1969), Brown and Liu, (1982) and Liu et al. (1979) were used to reduce the hourly-averaged sensor height winds to 10-meters. These profiles were found to give similar but not identical results, while the on-board reduction algorithm generally over-reduced the wind speeds compared to the similarity theory based profile models. In this study, we also examined a profile called the NPD (Norwegian Petroleum Directorate) proposed by Anderson and Lovseth (1993), who fitted a log-linear profile with Charnock roughness to profile data within the 10 m to 45 m height range. The data were obtained from a triangle of thin masts with sensor height range 10-100m located off the west coast of Norway (the so-called "Froya" database). Figure 2 shows the wind speed ratio Umeas/U10 as a function of wind speed for neutral conditions predicted by the Cardone (WindFN), Liu and NPD profiles as well as the constant on-board reduction factor used on the platform for Ekofisk and Gullfaks. The profile laws agree fairly closely with each other, while again the on-board reduction seems to over-reduce the wind speeds. At Ekofisk and at 20 m/s, the difference between Liu and NPD is less than 0.4 m/s. At Gullfaks and at 30 m/s the differences are closer to 1 m/s. WindFN lies between NPD and Liu and seems like a good compromise to use for the reductions in this study until a more precise profile applicable to heights up to 150 m can be developed. However, this exercise suggests that the reduction process itself imparts an uncertainty of about 2% to 3% in the reduced platform winds in the wind speed range of interest here.

The platform wind data were processed twice to effective neutral 10m winds: first, assuming neutral stability and second using the full stability dependent profile form. The second dataset was about 13% smaller than the first because air and sea temperature were not always available. Results from the stability-adjusted dataset are reported here.

As noted above, the QS data are from the most recently available NASA JPL Level II science file as processed using DIRTH. Retrievals flagged for land, rain or ice were not included in our analysis. The collocation process seeks the single nearest QS cell hit within a 100-km by 100-km box centered on the platform within a +/- 30-minute time window of the platform wind. Both standard matched-pair difference statistics and wind speed probability distributional comparisons in terms of quantile-quantile (Q-Q) scatter plots were produced for each platform and all platforms combined. Table 2 gives the paired-difference statistics by platform and all platforms combined. For the stability dependent reduction cases, the number of comparisons ranged from 3,172 at Ekofisk to 3,848 at Draugen with 18,500 combined collocations. The statistics in Table 2 show similar skill at each site. Over the combined collocations, the mean difference (QS-Plat) is 0.62 m/s, standard deviation of the difference is 1.76 m/s, the scatter index is 0.20 and the correlation coefficient is 0.93. The positive bias originates mainly from pairs with wind speeds of 5 m/s or lower. The wind direction scatter is 28.7 degrees. These statistics are only slightly worse than indicated from global buoy comparisons (e.g. Ebuchi et al., 2002), which also tend to be based on tighter spatial collocation filter (e.g. 25 km for Ebuchi et al. buoy collocations vs. effectively 50 km for our comparisons).

The distribution comparisons in terms of Q-Q plots, produced only from the collocation dataset, are very similar at all platforms showing, except for slight positive bias in QS light winds, a nice linear and accurate relationship between the QS and platform distributions up to the 99.9 percentile, which for most platforms is in the vicinity of about 25 m/s. Figure 3 gives the Q-Q plot for all platforms combined and also shows the Q-Q when the platform 10-m wind speeds are taken from the on-board reduction. This plot provides further evidence that the standard on-board reduction is too strong.

The winters sampled by QS in the North Sea contain fewer severe storms (through December 2002) than the NSCAT sampling period and, in fact, there are only 26 collocations found to date when either the QS or platform had wind speeds at 10 m exceeding 25 m/s. The QS and platform winds for these "hits", all in the range 25 m/s to 31 m/s, are compared in Table 3. The mean difference and standard deviation are -0.24 m/s and 2.6 m/s respectively with scatter index of 10%. The mean difference is within the uncertainty in the reduction method noted above and the skill in the retrievals is obviously very high.

There was one very severe storm of interest in the North Sea during the period studied; namely, the so-called "North Sea Hurricane of December 3, 1999". QS measured peak wind speeds of 35 m/s in the southwest quadrant of the storm, closely matching the maximum wind speed measured as this quadrant of the storm 3-hours after the QS pass crossed the position of a slender tower moored offshore northern Denmark in the Horns Rev wind farm. Winds and other meteorological variables, sampled at 1Hz, were recorded continuously at heights above sea level of 15 m, 30 m, 45 m, and 62 m. The maximum 10-minute mean wind speed recorded at the 62 m height was 45 m/s. Figure 4 shows the time series of 30-minute average wind speed and direction reduced to 10 m from the various anemometers at various heights using WindFN. The reduction from the best exposed anemometer (62m) is taken to be the best estimate of the time profile of 10-m wind speed and this provides a maximum sustained 10-m wind speed of 34 m/s. This comparison is not included in the table because of the time shift.

Table 4 compares the skill in QS overall found from the buoy comparisons of Ebuchi et al. (2002) over the whole wind speed range and our comparisons overall and for a subset greater than 20 m/s. Overall, the platform wind statistics, while showing skillful retrieval of winds by QS in this harsh environment, are slightly worse than shown by the buoy comparisons, possibly because of the larger spatial filter used in this study. Nevertheless, in over 12,000 collocations the QS wind speeds and directions easily exhibit the design skill levels for the instrument up to the highest winds sampled (35 m/s) and the bias in wind speed is comparable (at about 3%) to the uncertainty in the reduction of wind speeds from anemometer heights of the order of 100 m to 10 m with the best current surface boundary layer wind profile models. For the data pairs with either QS or the platform reporting wind speed above 20 m/s, as included in Table 4, the bias is -0.08 m/s (QS lower than platform), the standard deviation of the difference is 2.5 m/s and the scatter index, expressed as a percentage is 12%.

We conclude that QS data are useful and accurate to at least 35 m/s (at least in rain free areas) and may be used to diagnose the time and space evolution of the surface wind field in intense ocean storms, to assess the extreme marine surface wind speed climatology on a global basis and to improve surface wind and ocean response analyses and forecasts.

3. ERRORS IN REANALYSIS MARINE SURFACE WIND PRODUCTS

The 10-m global marine fields produced by the NRA project without doubt represent a significant improvement over earlier archived historical marine wind field databases. The direct application of these winds to a 40-year global deep water hindcast (Cox and Swail, 2001) provided the most accurate and homogeneous global wave climate specification produced to that date and a very useful database for studies of wave climate trend and variability (e.g. Wang and Swail, 2001). Nevertheless, detailed evaluation of the NRA winds in anticipation of the AES40 project showed the winds to be susceptible to significant improvements (Swail and Cox, 2000) especially for hindcasting of event peaks when the NRA surface winds are kinematically reanalyzed with the aid of interactive techniques in general, and, for tropical storms specifically, with a proven tropical cyclone wind model. Figure 5 compares the systematic error of deep water significant wave height (HS) hindcasts driven by unadjusted NRA winds (GROW) and reanalyzed NRA winds (AES40). The bias in HS in GROW hindcasts above 7 m is eliminated or at least greatly reduced in the AES40 hindcasts. The same general level of bias in winds and resulting waves seem to characterize the ERA40 products as well (Caires et al., 2004). However, thousands of analyst-hours were expended in the improvement of AES40 wind fields so this approach is not readily extendable to the globe. QS provides an opportunity to produce a reference dataset of global marine wind fields of unprecedented accuracy for the past five years as well as a basis for improvement of existing NRA and ERA40 products.

4. IMPACT OF QuikSCAT ON WAVE HINDCASTS

4.1 Direct Assimilation of SeaWinds

The QS real-time data stream is already being assimilated into real time NWP products at major centers (e.g. NCEP, ECMWF) and non-real time data are processed at Jet Propulsion Laboratory (PO.DAAC, 2001) where they are used to produce gridded daily and monthly mean wind fields. The University of Colorado use the final QS data to enhance NRA 6-hourly wind fields to produce new wind fields known as CORA winds (Milliff et al., 2004). In addition, dozens of studies have been published that demonstrate the incremental value of QS data to research on regional wind phenomena and air-sea interaction. This body of work has not produced a reanalysis gridded wind product of sufficient accuracy and resolution in space and time for most wave hindcasting purposes. We have recently carried out a global wave hindcast experiment with the CORA winds and find; unfortunately, that they lead to significantly biased wave hindcasts.

For the purposes of this pilot demonstration of the impact of QS enhanced wind fields on wave hindcasting skill, we have utilized the DIRTH processed winds to produce wind fields using OWI’s Interactive Kinematic Objective Analysis (IOKA) method (Cox et al., 1995) at 6-hourly wind fields over the entire South Atlantic Basin for one year. This basin is very important for practical purposes because it includes two of the most important new frontier areas of offshore energy production, West Africa and Brazil. This approach utilizes an interactive graphics wind work station (WWS). Figure 6 shows the data available at 12-hourly intervals (0600 UTC and 1800 UTC). The QS data essentially resolve the active wind field features between 25° S and 55° S. The main tasks of the analyst are to identify and remove areas where the QS algorithm selected the wrong aliases (this is rare), to interpolate the QS data rich information into the small inter-swath areas within a given map and to apply kinematic continuity principles to move information from the QS data rich synoptic time to the intermediate synoptic times (i.e. the 0000 UTC and 1200 UTC analyses).

Figures 7, 8 and 9 compare the hindcast made with these NRA/QS enhanced wind fields with hindcasts made with pure NRA winds. The ODGP2R spectral model was used in deep water mode on a grid of spacing 0.3125 latitude by 0.625 longitude. Figure 7 gives the pattern of mean difference between hindcast HS and satellite altimeter HS. Figure 8 gives the hindcast-altimeter distributional comparisons and Table 5 gives the matching statistics for the mid-latitude South Atlantic. These figures show there is a reduction in bias overall but especially so at the higher non-exceedance probabilities of 80% - 99.9 %. This characteristic of the pure NRA hindcast would greatly degrade the accuracy of derivative wave extremes for design. For illustrative purposes only, Figure 9 compares the Weibull distribution extrapolation to the 99% annualized non-exceedance probability of HS from the NRA and NRA/QS hindcast time series at selected grid locations offshore West Africa. The significant impact of QS on design levels is obvious at all latitudes.

4.2 QuikSCAT – NRA Wind Comparisons

How can we utilize QS wind products to improve the pre-QS multi-decade reanalysis products? In this section we describe briefly, with examples, a simple and evidently effective technique to minimize systematic errors in the NRA. The technique involves comparison of the NRA wind fields and the multi-year QS database of 25-km resolution winds, which typically provides in any marine region at least two observations per day taken at the times of the local ascending and descending passes. While our first attempts utilized the NASA JPL Level 2B product we have found the DIRTH products to be less noisy and somewhat more successful at filtering rain-contaminated cells. We use the JPL quality control flags to filter backscatter measurements probably contaminated (for the purposes of wind retrieval) by sea ice, rain or proximity to land. As shown above, we consider that over the wind speed range from 2 m/s to about at least 35 m/s the filtered wind speeds are accurate to within +/- 2 m/s and the wind direction is accurate to within +/- 20 degrees.

The comparative analysis consists of forming a matched QS/NRA wind vector dataset for each NRA grid box. In practice we apply a median filter to select a QS observation from each pass within a radius of 55-km from the NRA grid point. To account for the asynoptic nature of the satellite data, the NRA 6-hourly winds straddling a satellite observation are linearly interpolated in time to the hour nearest the time of the satellite observation. Given the time-matched dataset in each box over the overlapping data sample, the analysis proceeds to compare the two datasets using Oceanweather's TIMESCAT program for various stratifications of the matched pairs. The stratifications usually applied are season and wind direction, where the direction sectors may be defined in terms of unique or overlapping quadrants, centered on or offset from north. The directional binning is based on the NRA wind direction.

TIMESCAT generates two types of statistics. The first type consists of standard difference statistics on the matched data pairs of wind speed and direction including mean difference, rms difference, standard deviation of difference, scatter index and correlation coefficient. This type of comparison emphasizes the skill (or lack thereof) with which the NRA wind fields simulate the true time and space varying winds. The second type of comparison is applied to wind speed only and involves the comparisons of exceedance distributions computed separately from the NRA and QS data but using only data contained in the matched dataset. Specifically, the probability distributions of the NRA and QS wind speeds are compared in terms of Q-Q scatter plots. This type of comparison emphasizes the systematic differences between the NRA and the true winds within the stratification addressed. If the Q-Q plot shows a linear relationship between the distributions, then a simple correction algorithm for the systematic effects shown on the Q-Q plots is provided by the regression line through the data points.

Figure 10 gives a typical example of this type of comparison from a study recently conducted over the eastern North Pacific Ocean for the U.S. Army Corps of Engineers. The example applies not just for a single NRA box but over all NRA grid boxes within the zonal band between 40° N and 50° N and between the International Date Line (IDL) and 130W longitude (zonal variations were found to be small within this band). This figure shows the annual directionally stratified Q-Q scatter comparisons as four plots and the difference statistics in the table below the plots. The number of comparisons available in each direction bin of course depends on the wind climatology. There are over 120,000 data pairs in the westerly quadrant and less than 50,000 pairs in the northerly quadrant. The bias in NRA wind speeds is generally negative (-0.61 m/s over all data-pairs) but the skill is high as the correlation coefficient varies by quadrant between 0.82 and 0.90. Especially for the westerly and southerly quadrants, the Q-Q scatter plots show a clear tendency for two systematic wind speed error regimes, one in the range of non-exceedance probability 1-99% and the second in the range of 99%-99.9% with the wind speed break between these regimes in the 15 m/s to 20 m/s range. Earlier studies with Level 2B data tended to obscure the upper range because of noise in the retrievals and apparently failure of the quality flag to successfully filter all rain-contaminated cells in storm conditions associated with the stronger winds. For this particular study we adopted a piecewise continuous double linear regression to adjust the NRA winds. Interestingly, this type of correction seems to mimic well the tendency for interactive kinematic analysts to focus on and apply greater corrections to the regions with wind speeds greater than 15 m/s. NRA wind directions are also corrected based in the mean direction biases shown in the table.

Figure 11 shows the effectiveness of the above type of correction procedure when applied over the entire year 2000 to the whole of the eastern North Pacific in terms of the spatial variation of NRA-QS differences of the 90th percentile wind speed. The adjustment procedure is especially effective at reducing large negative biases in NRA wind speeds in the trade winds between 0-10° N and in the coastally enhanced northwesterly flows off the coast of California (note that in the coastal zone of the eastern North Pacific, NRA grid point specific adjustments were derived and applied). Finally in Figure 12 we show an example of the effects of the adjustments on the wind field surrounding an extratropical cyclone in the Gulf of Alaska. Note the significant enhancements of the surface wind speed in the jet streaks southeast and northwest of the center and the improved agreement between the QS enhanced winds and the buoy wind measurements. The impact of these enhanced North Pacific wind fields on wave hindcast of this test year are discussed at this conference by Hansen and Jensen (2004).

OWI now routinely apply the approach described in this section to develop NRA/QS enhanced wind fields to drive long term regional wave hindcasts for the purposes of developing design wave datasets. Figure 13 shows some examples of the skill achieved in the distribution of HS including the Sea of Okhotsk, South China Sea, Irish Sea, and offshore Algeria. The corresponding statistics are provided in Table 6.

5. DISCUSSION

The proof of concept that spaceborne scatterometers could monitor the evolution of synoptic scale marine surface marine wind fields virtually continuously was demonstrated by the prematurely aborted SEASAT mission in 1978. And yet, more than two decades would pass before the launch of a satellite, namely QuikSCAT that provides accurate daily global coverage by an advanced scatterometer. By July 2004 a five-year dataset had been collected and it continues to grow. This dataset is of great value for the purposes of ocean response model forcing and its temporal and spatial resolution seem especially appropriate for forcing of wave models. In this study we have demonstrated how the QS data may be utilized directly to develop very accurate synoptic wind fields for wave models. Unfortunately, there has not evolved yet an accurate purely objective and automated analysis system for the assimilation of QS data into a background field but until such a system is developed, the data are quite amenable to incorporation in interactive objective kinematic analysis systems such as OWI's IOKA system. We are currently producing a 5-year global marine wind dataset in this manner, a prodigious but not prohibitively formidable task. This paper demonstrates the positive impact of such wind fields on wave hindcasting in the hitherto data-void South Atlantic basin. In addition, we have shown how the QS data may be used to quantify and minimize systematic errors in products of existing multi-decade reanalysis projects. This approach has already been used at OWI to provide accurate long term wind and wave hindcast datasets for several regional basins for the purposes of derivation of normal and extreme wave climate statistics. We are currently extending this approach to produce our third and hopefully final version of GROW. While the results presented herein were provided by existing well-calibrated second and third generation wave prediction models and the results appear accurate enough for most engineering applications, there remains much work to be done to develop a wave prediction model suitable for use in deep and shallow water whose source terms derive from first principals of physics and are free of arbitrary tuning coefficients. A significant benefit of the QS dataset is that it enables the specification of reference wind fields of sufficient accuracy to be used in such future fundamental wave model development and validation research.

REFERENCES

Andersen, O. J. and J. Lovseth, 1993: The Froya data base for gale force maritime wind. Structural Dynamics-EURODYNE'93. Moan et al. (eds), Balkema, Rotterdam, ISBN 90 5410 336 1, p. 1091-1097.

Bourassa, M. A., D. M. Legler, J. J. O'Brien and S. R. Smith, 2003: SeaWinds validation with research vessels. J. Geophys. Res., 108, C2, I1-I16.

Brown, R. A. and T. Liu, 1982: An operational large-scale marine planetary boundary layer model. J. Appl. Meteor., 21, 261-269.

Cardone, V. J., 1969: Specification of the wind distribution in the marine boundary layer for wave forecasting. Report TR 69-1, New York University. Available from NTIS, Order No. AD 702 490.

Cardone, V. J., H. C. Graber, R. E. Jensen, S. Hasselmann, and M. J. Caruso, 1995: In search of the true surface wind field in SWADE IOP-1: Ocean wave modeling perspective. The Global Atmosphere and Ocean System, 3, 107-150.

Cardone, V. J., R. E. Jensen, D. T. Resio, V. R. Swail, and A. T. Cox, 1996: Evaluation of contemporary ocean wave models in rare extreme events: Halloween storm of October 1991; Storm of the century of March, 1993. J. of Atmos. and Oceanic Tech., 13, 198-230.

Cardone, V. J., E. A. Ceccacci, A. T. Cox and J. G. Greenwood, 2000: Accuracy of scatterometer winds assessed from in-situ measured wind data up to 32 m/s. Paper No. OS52A-03. 2000 Spring Meeting of American Geophysical Union. Washington, DC.

Cardone, V. J., A. T. Cox, K. A. Lisaeter and D. Szabo, 2004: Hindcast of winds, waves and currents in Hurricane Lili (2002). Proceedings of Offshore Technology Conference, May, 2004, Houston, TX.

Caires, S., A. Sterl, J.-R. Bidlot, N. Graham and V. R. Swail, 2004: Intercomparison of different wind-wave reanalyses. J. Climate, 17 (10), 1893-1913.

Cox, A. T., J. A. Greenwood, V. J. Cardone and V. R. Swail. An Interactive Objective Kinematic Analysis System Fourth International Workshop on Wave Hindcasting and Forecasting. October 16-20, 1995. Banff, Alberta, Canada.

Cox, A. T. and V. R. Swail, 2001: A global wave hindcast over the period 1958-1997: validation and climate assessment. JGR (Oceans); 106, C2, 2313-2329.

Ebuchi, N, H. C. Graber and M. J. Caruso, 2002: Evaluation of wind vectors observed by QuikSCAT/SeaWinds using ocean buoy data. J. Atmos. Oceanic. Tech., 19, 2049-2062.

Freilich, M. H., D. G. Long, and M. Spencer, 1994: SeaWinds: A scanning scatterometer for ADEOS-II – Science overview. Proceedings of International Geoscience and Remote Sensing Symposium, Pasadena, CA, 960-963.

Hanson J. L. and R. E. Jensen, 2004: Wave system diagnostics for numerical wave models. 8th International Workshop of Wave Hindcasting and Forecasting. November 14-19, 2004. Oahu, Hawaii.

Huddleston, J. N. and B. W. Stiles, 2000: A multidimensional histogram rain-flagging technique for SeaWinds on QuikSCAT. IEEE Geosciences and Remote Sensing symposium, Inst. Of Elctr. and Electr. Eng., Honolulu, Hawaii.

Physical Oceanography DAAC. SeaWinds on QuikSCAT Level 3 Daily, Gridded Ocean Wind Vectors (JPL SeaWinds Project). NASA JPL Physical Oceanography DAAC, Pasadena, CA (2001), JPL PO.DAAC Product 109.

Liu, W. T., K. B. Katsaros and J. A. Businger, 1979: Bulk parameterization of air-sea exchanges of heat and water vapor including the molecular constraints at the interface. J. Atmos. Sci., 36, 1722-1735.

Milliff, R. F., J. Morzel, D. B. Chelton, and M. H. Freilich, 2004: Wind stress curl and wind stress divergence biases from rain effects on QuikSCAT surface wind retrievals. J. Atmos. and Oceanic Tech., 21, 1216-1231.

Moon, I.-J., I. Ginis, T. Hara, H. L. Tolman, C. W. Wright, and E. J. Walsh, 2003: Numerical simulation of sea surface directional wave spectra under hurricane wind forcing. J. Phys. Ocean. 33 (8), 1680-1706.

Powell, M. D., S. H. Houston, L. R. Amat and N. Morisseau-Leroy, 1998: The HRD real-time hurricane wind analysis system. J. of Wind Eng. and Ind. Aerodynamics, 77 & 78, 53-63.

Puskar, F. J., R. K. Aggarwal, C. A. Cornell, F. Moses, C. Petrauskas, 1994. A Comparison of Analytically Predicted Platform Damage to Actual Platform Damage During Hurricane Andrew. 26th Annual Offshore Technology Conference, Houston. Paper No. OTC 7473.

Swail, V.R. and A.T. Cox, 2000: On the use of NCEP/NCAR reanalysis surface marine wind fields for a long term North Atlantic wave hindcast. J. Atmos. Tech. Vol. 17, No. 4, pp. 532-545, 2000.

Taylor, P. K., E. C. Kent, M. J. Yelland and B. I. Moat, 1999: The accuracy of marine surface winds from ships and buoys. CLIMAR99: WMO Workshop on Advances in Marine Climatology, 8-15 September, 1999, Vancouver, CA, p. 59-68. Available from Environment Canada.

Wentz, F. J. and D. K. Smith, 1999: A model function for the ocean-normalized radar cross section at 14GHz derived from NSCAT observations. J. Geophys. Res., 104, 11499-11514.

Wang, X. L., Val R. Swail, 2001: Changes of Extreme Wave Heights in Northern Hemisphere

Oceans and Related Atmospheric Circulation Regimes. Journal of Climate: 14 (10), 2204–2221.

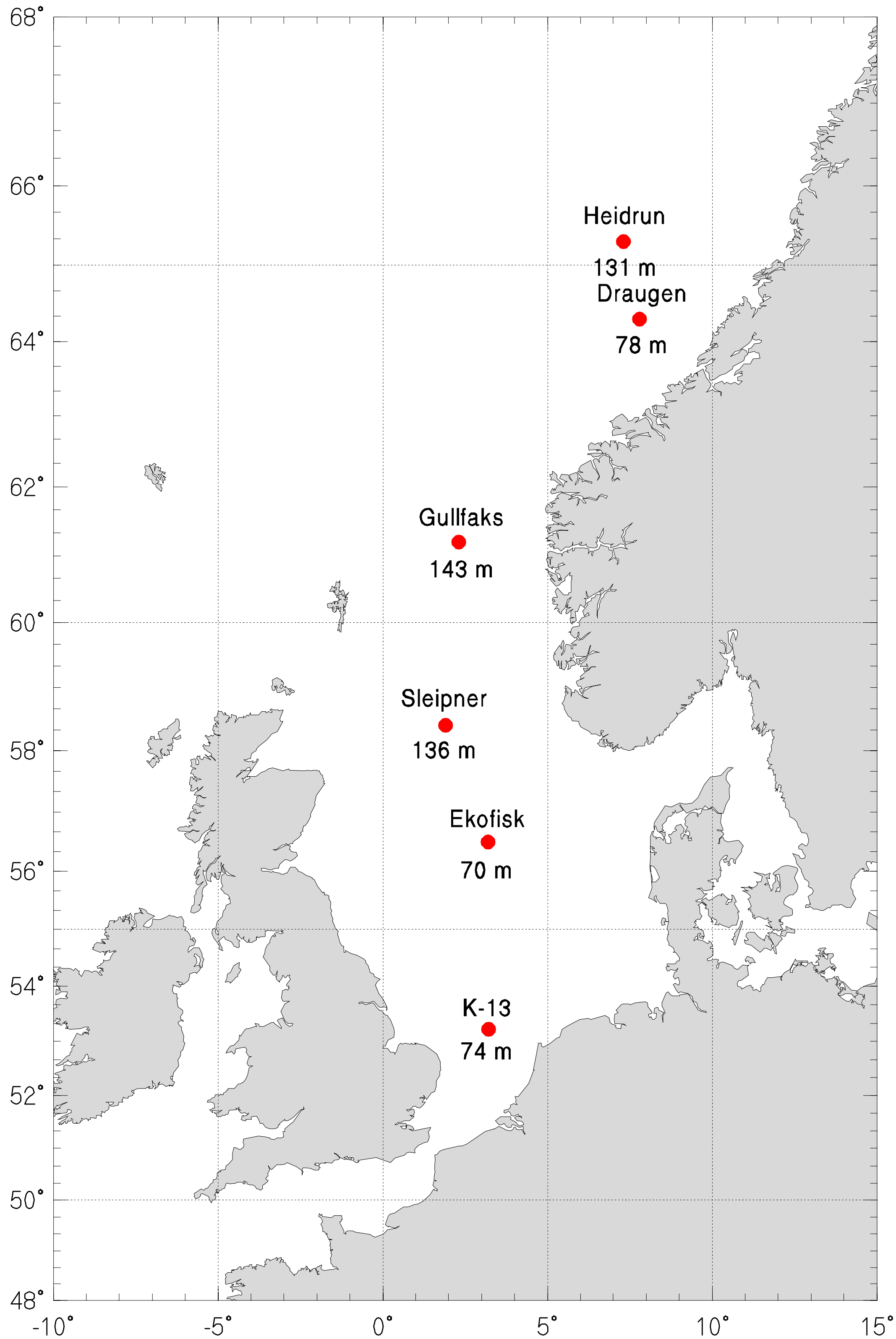

Figure 1: Platforms used to evaluate QuikSCAT winds (Anemometer height below name).

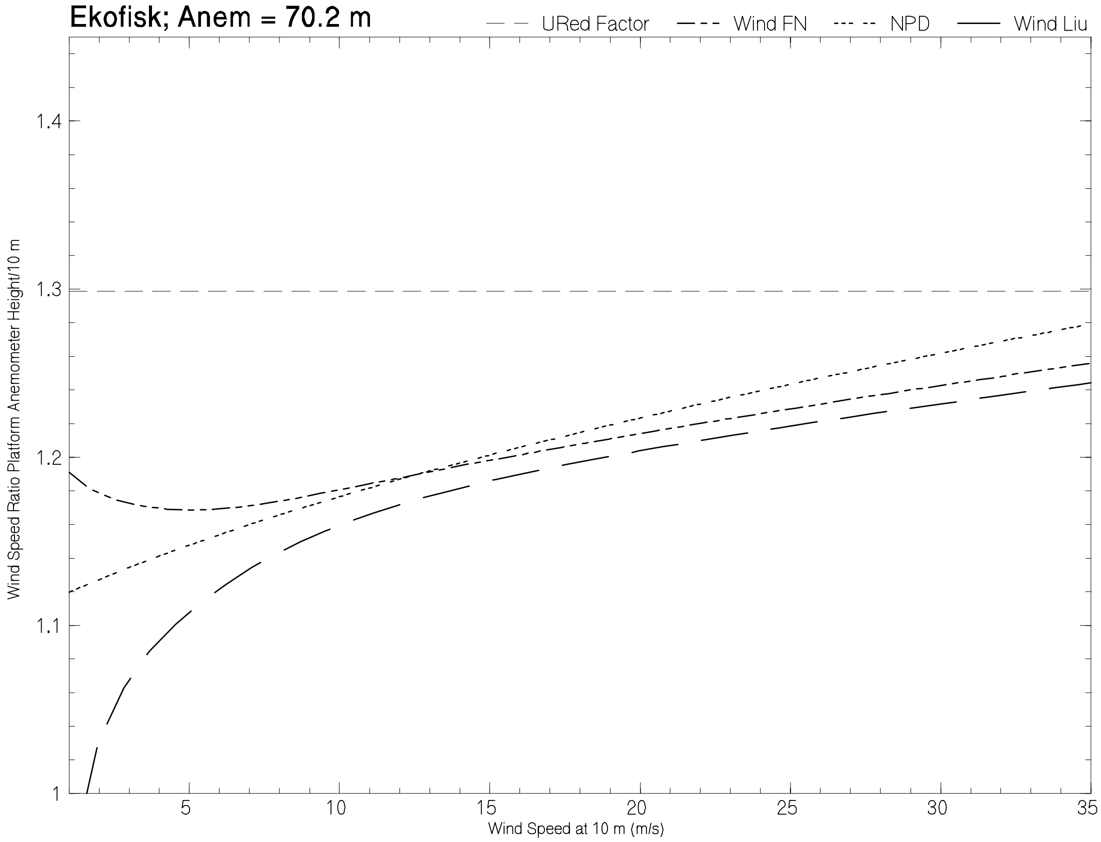

Figure 2 (a): Effect of reduction to 10 meters of alternative wind profiles at Ekofisk.

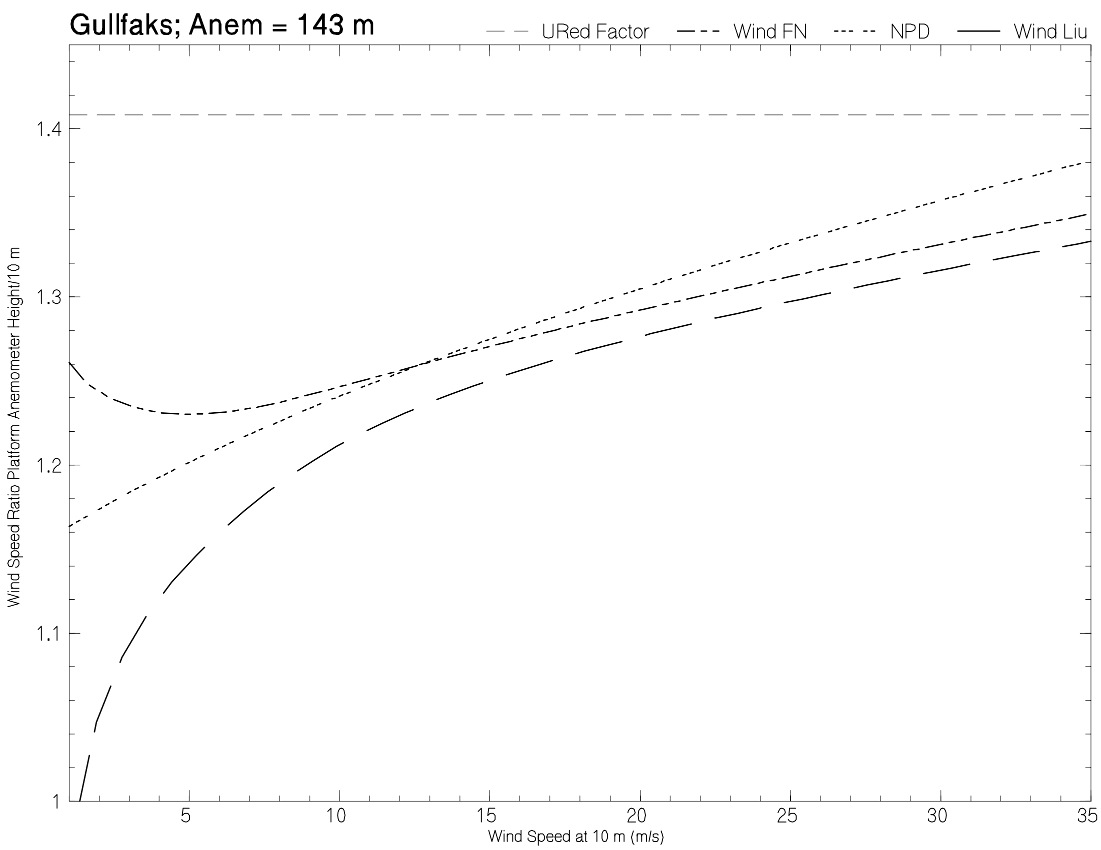

Figure 2 (b): Effect of reduction to 10 meters of alternative wind profiles at Gullfaks.

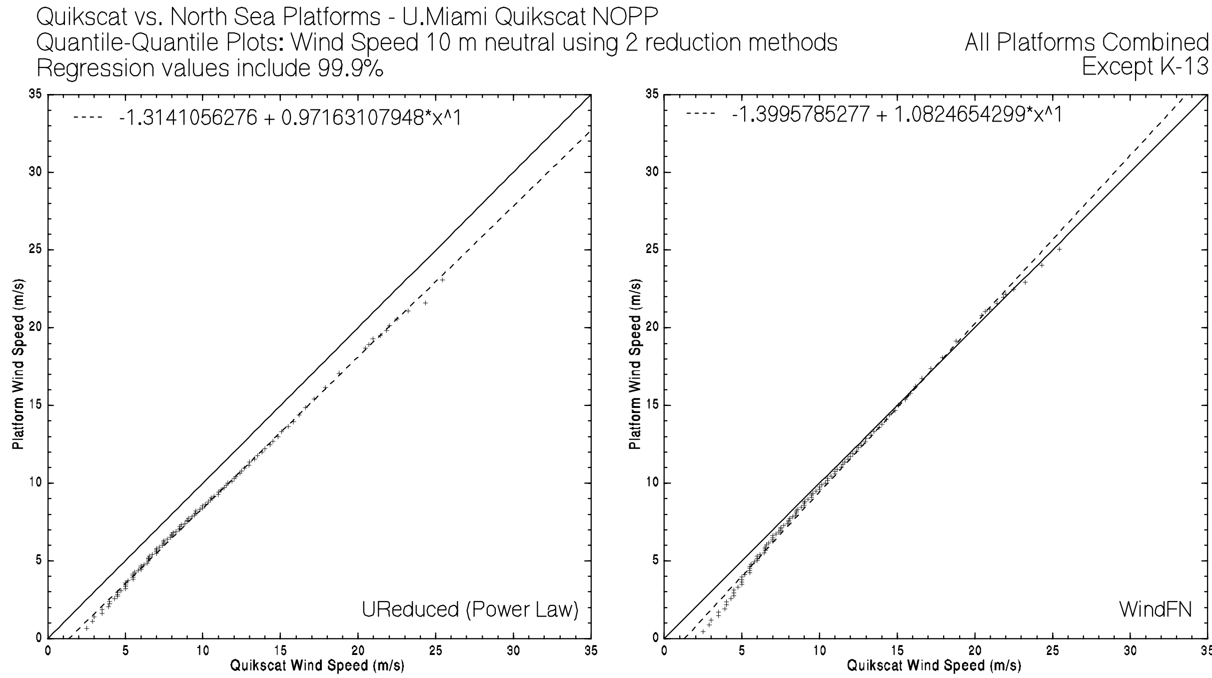

	Platform	Method	Number of Pts	Mean Plat	Mean QScat	Diff (Q-P)	RMS Error	Stnd Dev	Scat Index	Ratio	Corr Coeff
Wind Spd. (m/s)	All	URed	18500	7.50	9.07	1.56	2.31	1.70	0.23	0.85	0.91
Wind Spd. (m/s)	All	WindFN	18500	8.45	9.07	0.62	1.76	1.65	0.20	0.63	0.93
Wind Dir. (deg)	All	URed-FN	18491	243.28	231.38	-5.47	N/A	28.72	0.08	N/A	N/A

Figure 3: Comparison of collocated QuikSCAT and platform winds in terms of wind speed distributions as Q-Q plots (above) and difference statistics of matched pairs (below).

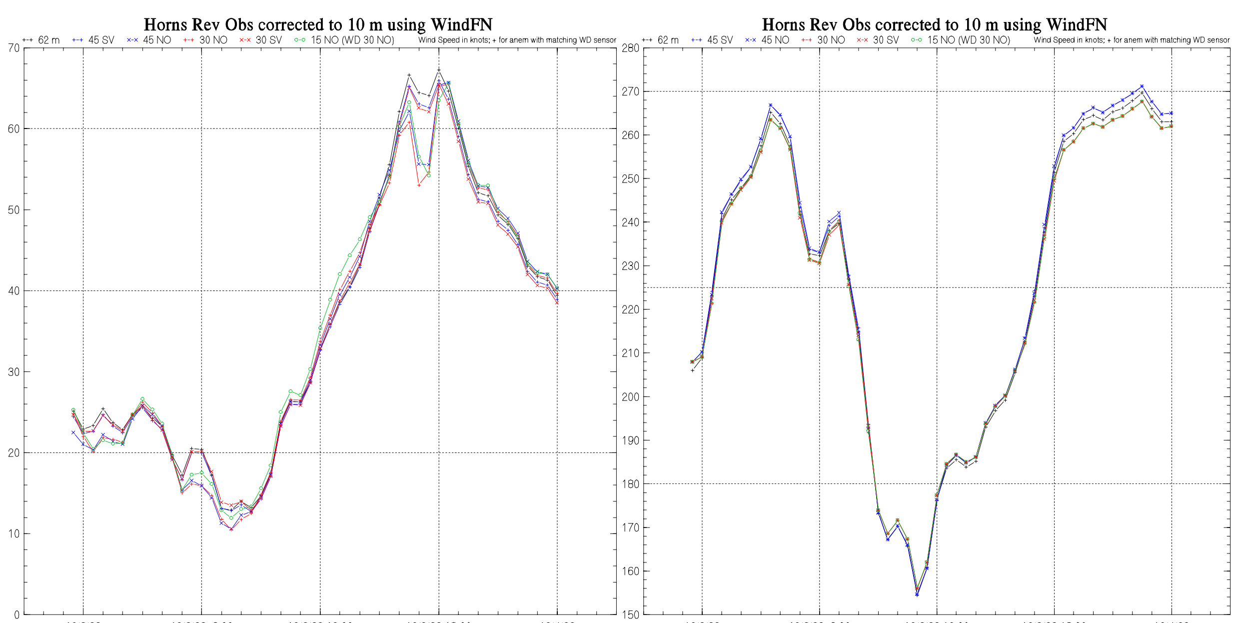

Figure 4: Measured winds at Horns Rev wind farm tower in North Sea “Hurricane” of 12/1999.

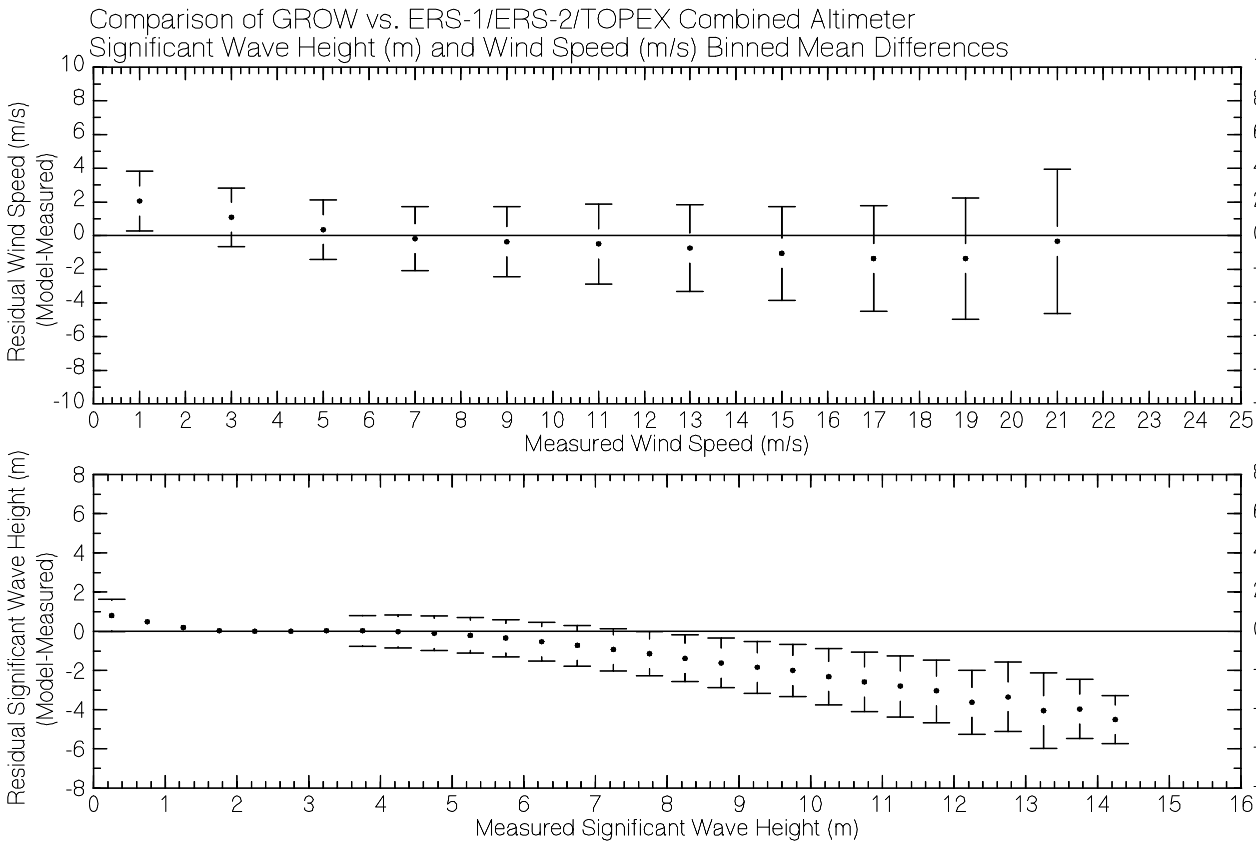

Figure 5 (a): Evaluation of hindcast (GROW) driven by NRA wind fields.

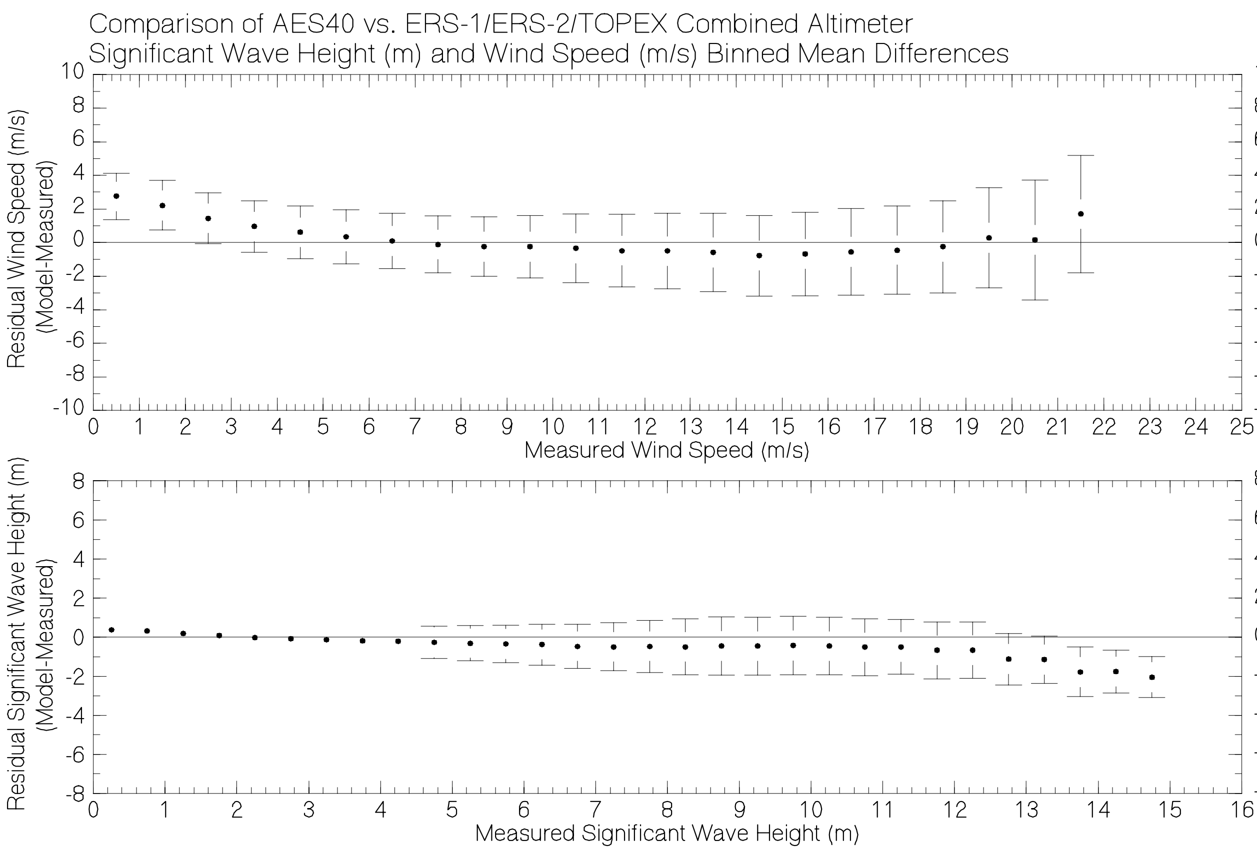

Figure 5 (b): Evaluation of hindcast (AES40) driven by reanalyzed NRA wind fields.

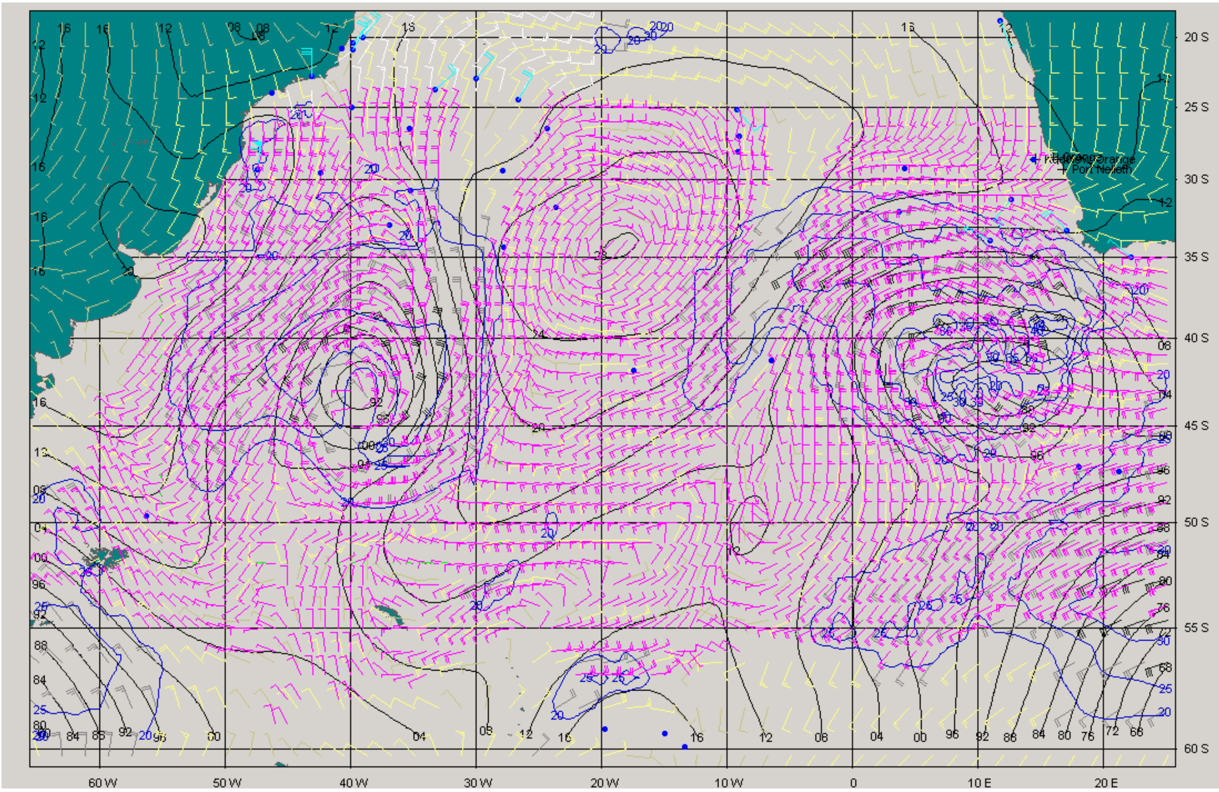

Figure 6: Sample “synoptic” QuikSCAT data (Pink barbs are QuikSCAT winds, variegated barbs are final winds, black lines are isobars every 4 millibars, blue lines are isotachs every 5 knots above 20 knots)

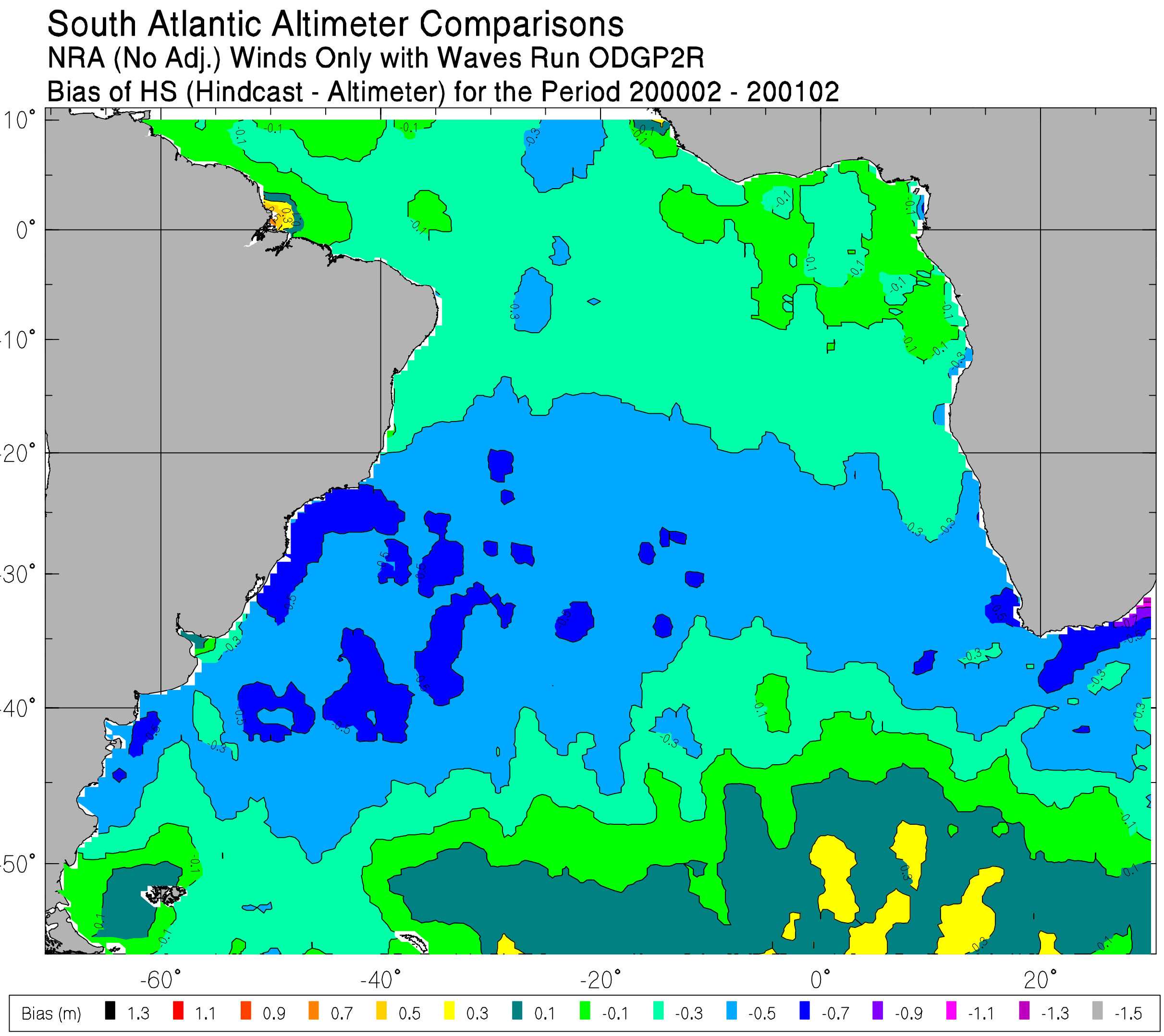
South Atlantic Altimeter Comparisons
NRA (No Adj.) Winds Only with Waves Run ODGP2R
Bias of HS (Hindcast - Altimeter) for the Period 200002 - 200102
10°
0°
-10°
-20°
-30°
-40°
-50°
-60°
-40°
-20°
0°
20°
Bias (m) 1.3 1.1 0.9 0.7 0.5 0.3 0.1 -0.1 -0.3 -0.5 -0.7 -0.9 -1.1 -1.3 -1.5

Figure 7 (a)

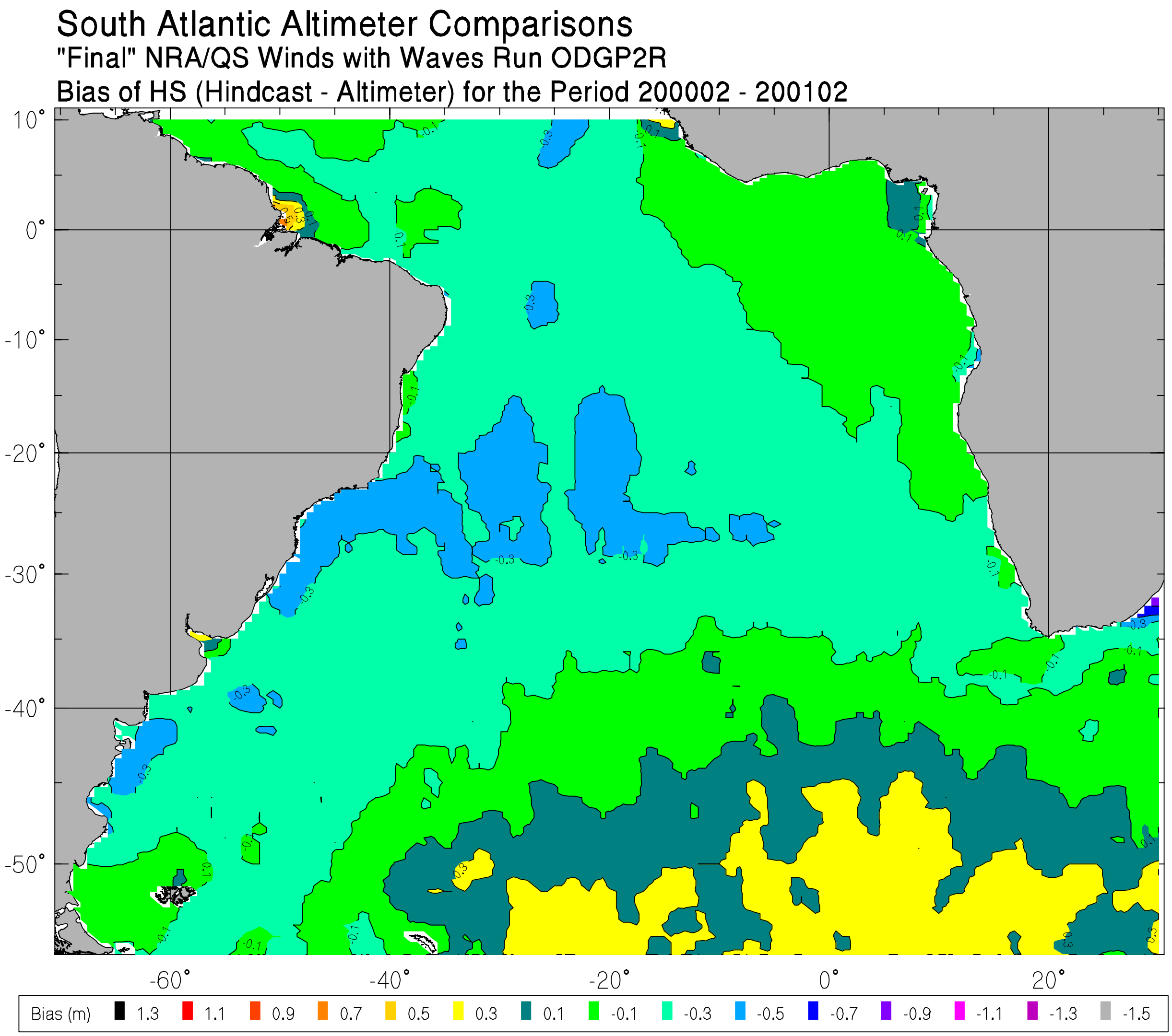
South Atlantic Altimeter Comparisons
"Final" NRA/QS Winds with Waves Run ODGP2R
Bias of HS (Hindcast - Altimeter) for the Period 200002 - 200102
10°
0°
-10°
-20°
-30°
-40°
-50°
-60°
-40°
-20°
0°
20°
Bias (m) 1.3 1.1 0.9 0.7 0.5 0.3 0.1 -0.1 -0.3 -0.5 -0.7 -0.9 -1.1 -1.3 -1.5

Figure 7 (b)

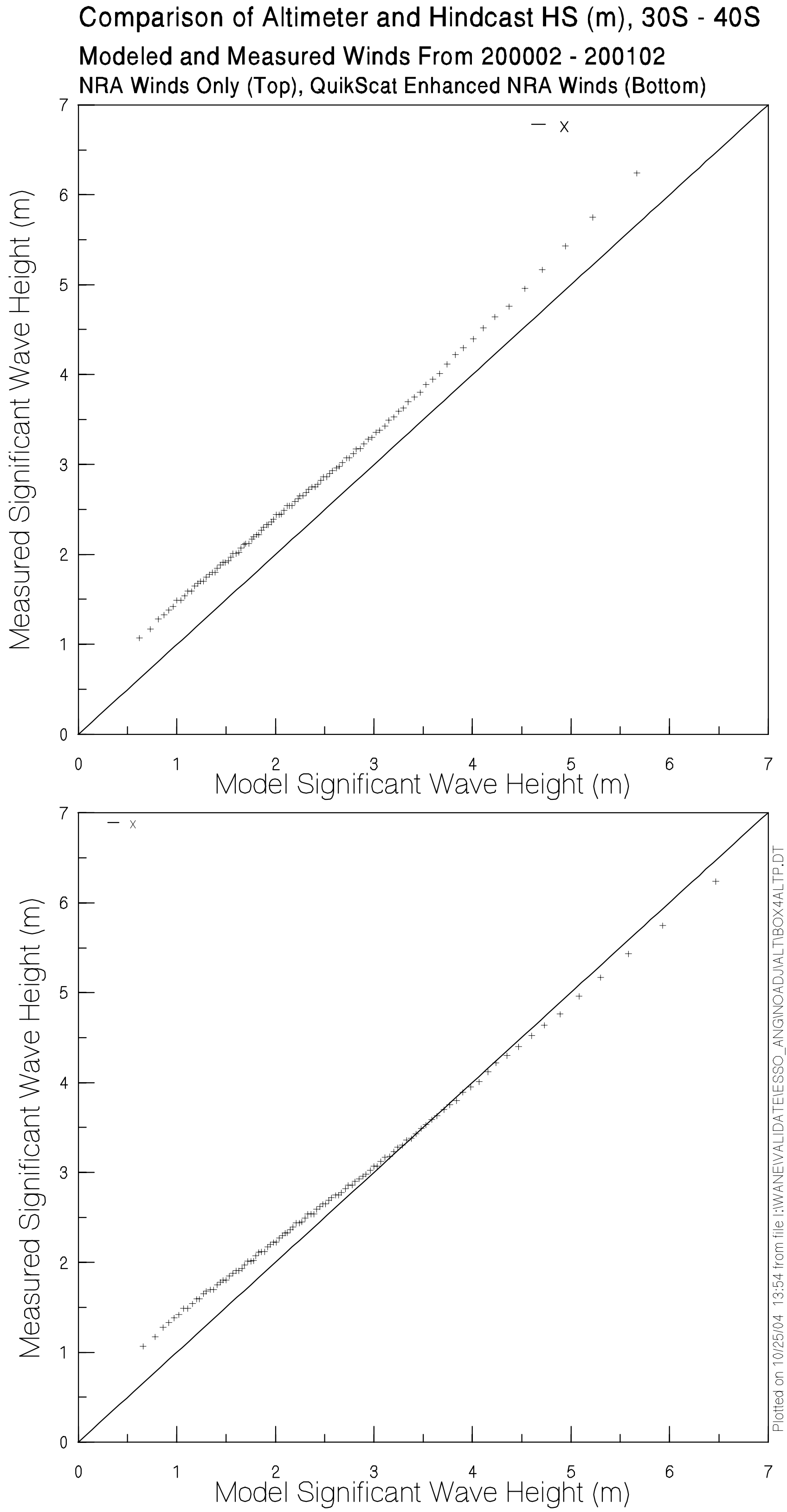
Comparison of Altimeter and Hindcast HS (m), 30S - 40S
Modeled and Measured Winds From 200002 - 200102
NRA Winds Only (Top), QuikScat Enhanced NRA Winds (Bottom)
Measured Significant Wave Height (m)
Model Significant Wave Height (m)
Measured Significant Wave Height (m)
Model Significant Wave Height (m)
Plotted on 10/25/04 13:54 from file I:\WANE\VALIDATE\ESSO_ANG\NOADJ\ALT\BOX4ALTP.DT

Figure 8

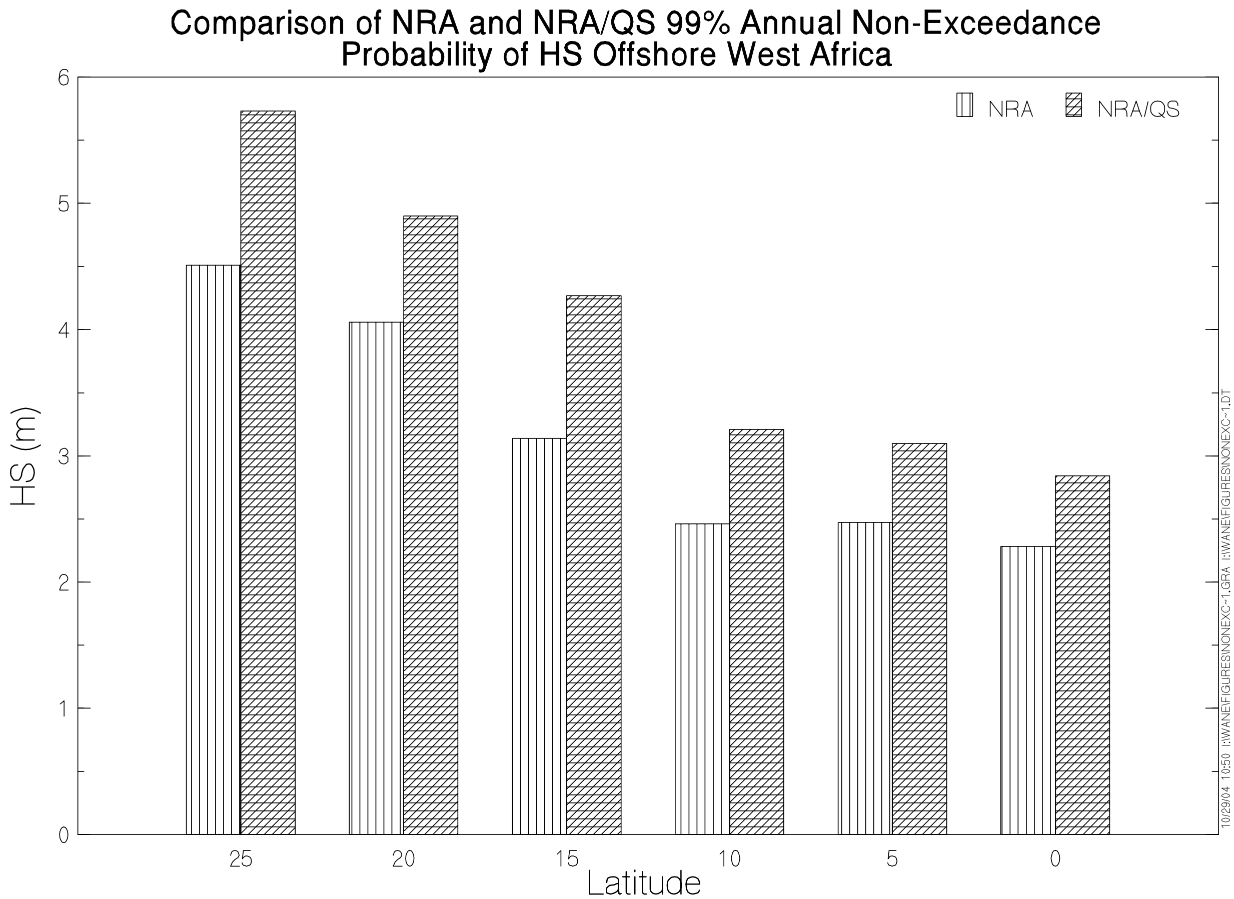

Figure 9

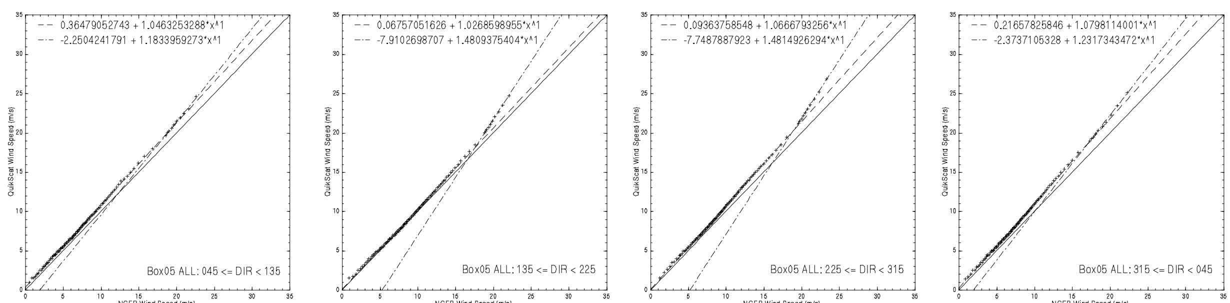

Hindcast Period ALL: 01-JUL-1999 00:00:00 to 30-JUN-2002 23:00:00

	Box	Month	Number of Pts	Mean Meas	Mean Hind	Diff (H-M)	RMS Error	Stnd Dev	Scat Index	Ratio	Corr Coeff		Number of Pts	Mean Meas	Mean Hind	Diff (H-M)	Stnd Dev	Scat Index
Wind Spd. (m/s)	Box05	ALLALL	274818	9.02	8.41	-0.61	2.18	2.09	0.23	0.39	0.87	Wind Dir. (deg)	274818	257.64	251.77	-1.19	23.38	0.06
Wind Spd. (m/s)	Box05	ALL045	27313	7.72	7.03	-0.69	2.50	2.40	0.31	0.41	0.82	Wind Dir. (deg)	27313	90.24	91.50	1.17	28.37	0.08
Wind Spd. (m/s)	Box05	ALL135	77872	8.92	8.62	-0.31	2.27	2.25	0.25	0.49	0.85	Wind Dir. (deg)	77872	188.80	189.98	1.47	26.22	0.07
Wind Spd. (m/s)	Box05	ALL225	122511	9.67	8.97	-0.70	2.05	1.93	0.20	0.35	0.90	Wind Dir. (deg)	122511	271.27	267.02	-3.94	19.42	0.05
Wind Spd. (m/s)	Box05	ALL315	47122	8.24	7.43	-0.81	2.13	1.97	0.24	0.33	0.87	Wind Dir. (deg)	47122	351.74	352.81	0.54	24.10	0.07

Figure 10: Systematic differences in wind speed between QS and NRA at 30° - 40° N in the eastern North Pacific for the indicated wind direction quadrants. The statistics of wind speed and wind direction differences for the individual QS-NRA matched pairs are shown below the wind speed Q-Q plots.

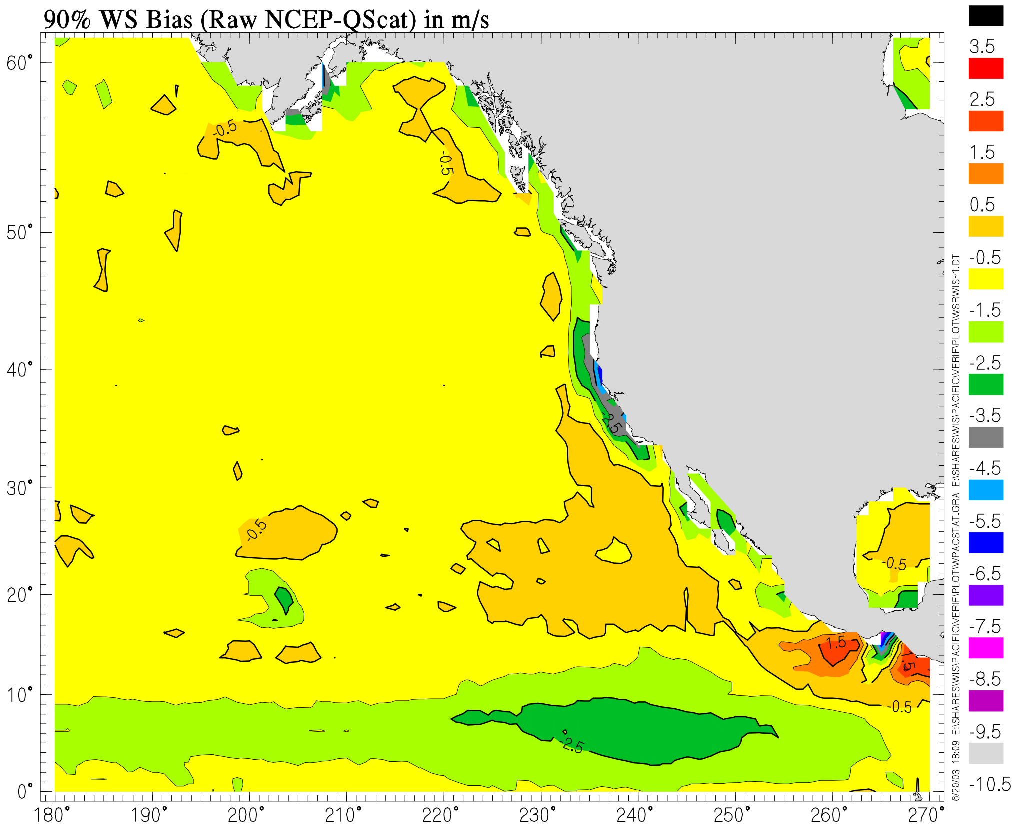

(a) Unadjusted

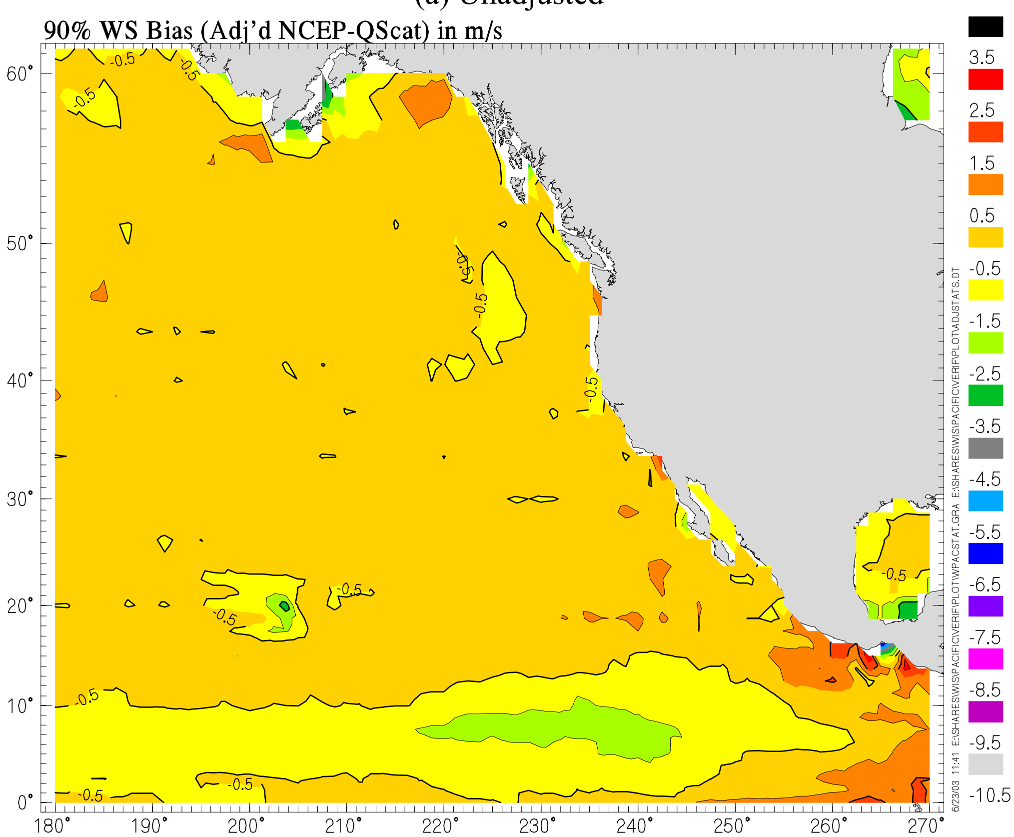

(b) Adjusted

Figure 11: Bias in 90th percentile wind speed (relative to QS) in pure NRA wind fields (above) and NRA adjusted using QS based regressions (below).

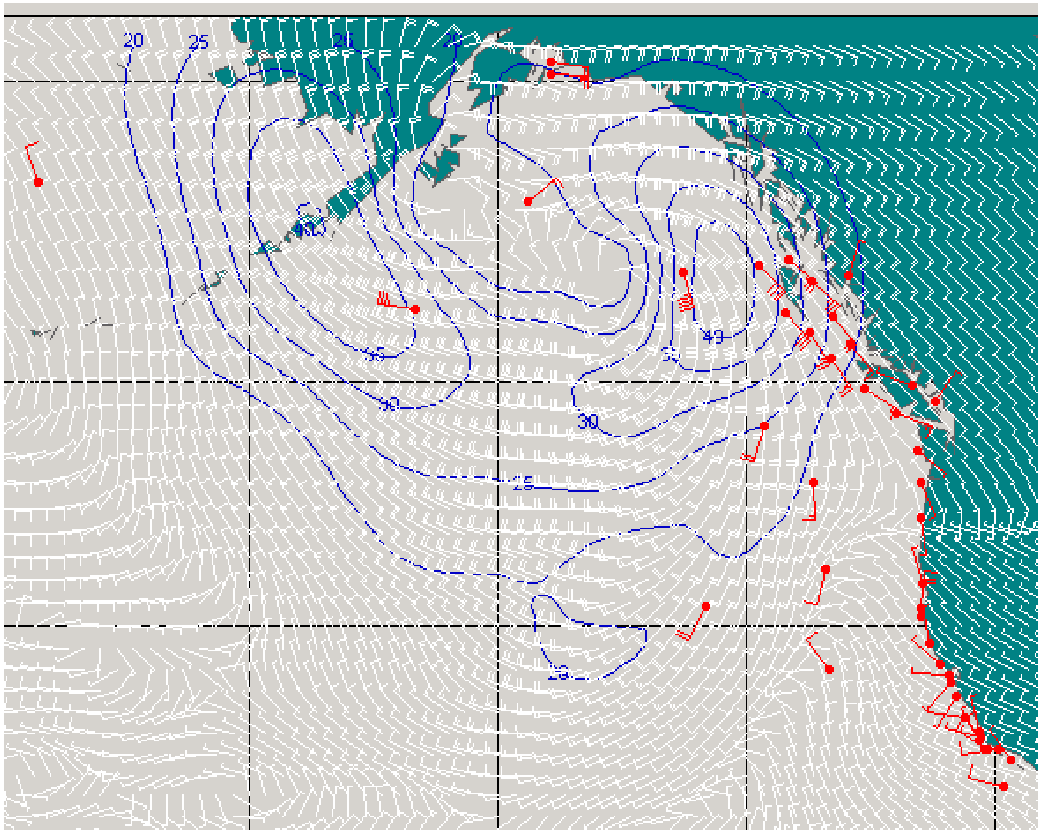

(a) Base Case Wind Field

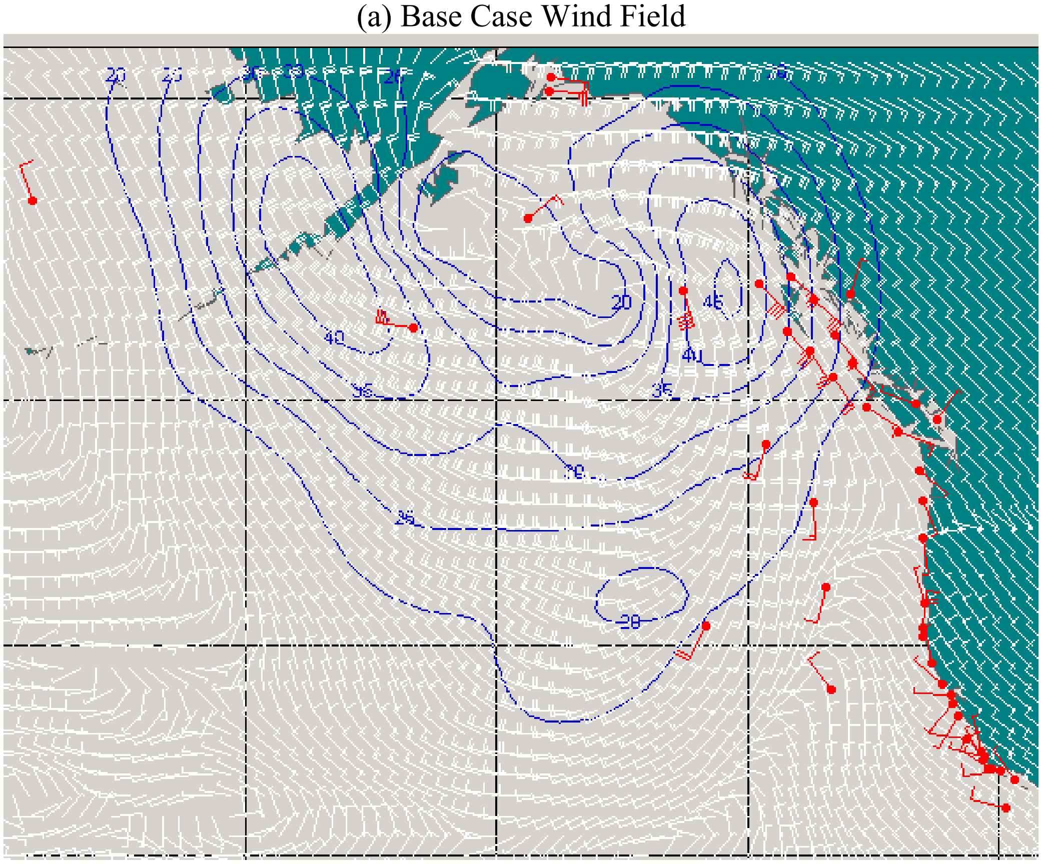

(b) Adjusted Wind Field

Figure 12: Comparison of Gulf of Alaska storm surface wind field in NRA winds (a) and NRA adjusted for systematic effects using QS based regressions (b).

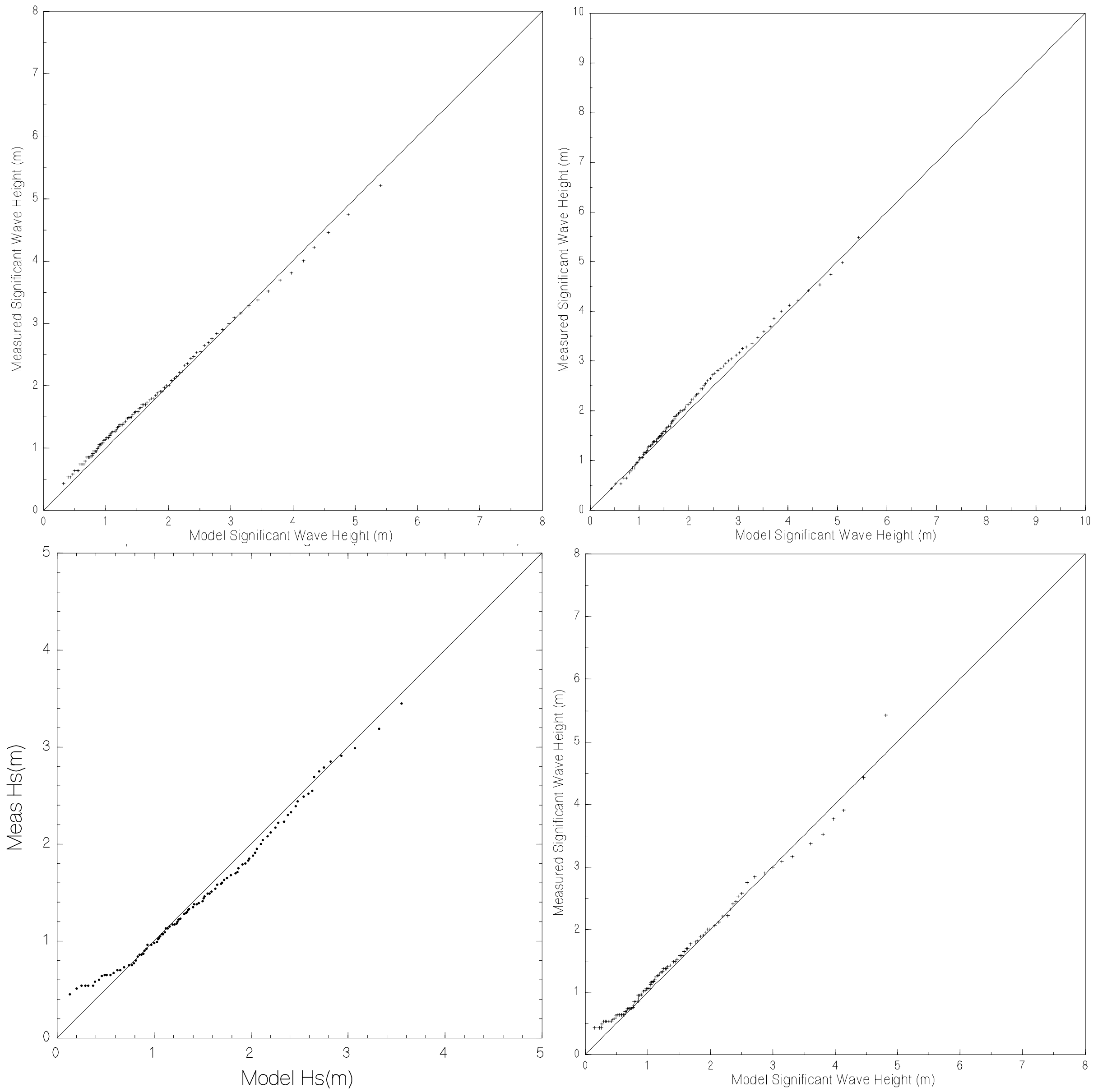

Figure 13: Examples of HS biases in terms of model vs. altimeter Q-Q scatter plots in hindcasts driven by QuikSCAT corrected wind fields (clockwise from top left: Sea of Okhotsk, South China Sea, offshore Algeria, and Irish Sea)

Table 1: North Sea Platforms Used to Evaluate QuikSCAT

Platform	**Location**	**Anemometer Height (m)**	**Water Depth (m)**	**Reduction Factor**	**Measurement Interval**
Draugen	64.3N 7.8E	78	251	0.77	199907-200212: 20 min
Ekofisk	56.5N 3.2E	116 & 70.2	70	0.73 & 0.77	199907-200212: 20 min
Gullfaks	61.2N 2.3E	143	217	0.71	199907-200106: 20 min 200107-200212: 10 min
Heidrun	65.3N 7.3E	131	350	0.72	199907-200112: 20 min 200201-200206: 10 min 200207-200212: 20 min
K-13	53.22N 3.22E	74	23	~0.81	199907-200212: 1-hr (WD last 10-min of preceding hour)
Sleipner	58.4N 1.9E	136	82	0.71	199907-200212: 20 min

Table 2: : Platform Winds Reduced to 10 m using Cardone 1969 (WindFN)

Platform	Wind Speed (m/s)								Wind Direction (deg)					
	No.	Mean Plat	Mean QS	Diff (Q-P)	RMS Error	Stnd Dev	Scat Index	Corr Coeff	No.	Mean Plat	Mean QS	Diff (Q-P)	Stnd Dev	Scat Index
Draugen	3848	8.29	8.46	0.17	1.77	1.76	0.21	0.93	3848	258.28	236.05	0.43	31.31	0.09
Ekofisk	3172	7.98	8.94	0.96	1.86	1.59	0.20	0.92	3171	238.08	235.38	-2.31	24.52	0.07
Gullfaks	3671	9.21	9.75	0.54	1.82	1.74	0.19	0.94	3662	245.61	215.55	-17.39	31.60	0.09
Heidrun	4481	8.24	9.07	0.84	1.70	1.48	0.18	0.94	4482	247.50	251.69	-4.45	26.28	0.07
K-13[1]	2954	8.14	8.32	0.18	1.73	1.72	0.21	0.90	2878	236.36	233.14	-3.75	25.96	0.07
Sleipner	3328	8.54	9.13	0.59	1.67	1.57	0.18	0.94	3328	237.43	226.84	-3.98	25.63	0.07
All[2]	18500	8.45	9.07	0.62	1.76	1.65	0.20	0.93	18491	243.27	231.38	-5.47	28.72	0.08

[1] K-13 statistics using potential wind speed profile by KNMI
[2] Except K-13

Table 3: Platform-QS Pairs where either exceeds 25 m/s

YYYYMM	DDHHMM	Platform	QuikSCAT WS	Platform WS	QuikSCAT WD	Platform WD
200001	291900	Sleipner	31.0	31.3	284.5	296.6
200111	301800	Gullfaks	27.1	27.2	150.2	176.8
200111	110400	Draugen	25.9	27.1	290.7	273.7
200111	102000	Heidrun	23.6	26.7	265.3	263.7
200010	301800	Ekofisk	22.0	26.7	210.0	245.0
199912	010300	Draugen	25.0	26.5	309.0	310.3
200010	302000	Draugen	23.6	26.0	83.5	90.0
200201	281900	Ekofisk	25.7	26.0	282.0	279.3
199911	301900	Sleipner	23.0	25.9	256.1	260.5
200002	231800	Gullfaks	26.7	25.9	172.7	183.0
200111	150400	Draugen	25.2	25.6	295.3	280.7
199912	010500	Draugen	23.0	25.4	316.0	304.7
200111	142000	Draugen	24.3	25.2	226.7	229.6
200111	102000	Draugen	25.3	25.2	265.5	270.6
200212	240500	Gullfaks	28.9	25.1	151.6	166.3
200212	240400	Gullfaks	26.0	25.1	150.6	164.4
200010	310300	Draugen	20.5	25.0	95.2	98.3
200111	110400	Heidrun	26.7	24.3	291.6	280.0
200202	141900	Draugen	27.6	24.1	230.7	225.0
200212	241800	Gullfaks	25.6	24.0	142.8	162.9
200212	231900	Gullfaks	27.8	24.0	155.4	167.8
200002	032000	Heidrun	25.7	23.9	213.2	203.7
199911	291900	Heidrun	26.0	23.7	255.8	255.2
200212	240400	Sleipner	25.1	23.4	132.1	132.7
200203	270300	Draugen	25.7	22.7	210.9	216.4
200212	200500	Draugen	25.7	20.5	12.4	0.0

Mean QuikSCAT WS: 25.49 m/s
Mean Platform WS: 25.25 m/s
Mean Difference (Q-P): -0.24
RMS: 2.60
Stnd Dev: 2.58
Scat Index: 0.10
Corr Coeff: 0.18

Mean QuikSCAT WD: 229.30 deg
Mean Platform WD: 233.32 deg
Mean Diff (Q-P): 3.31
Stnd Dev: 12.44
Scat Index: 0.04

Table 4: Comparison of Buoy and Platform QuikSCAT Validation

	No.	**Bias (Q-P)**	**RMS**	**Scat. Ind.**
Ebuchi et al. (2002)	48540	0.05	1.00	0.15
Platforms (all pairs)*	18500	0.62	1.76	0.20
Platforms (WS>20 m/s)*	313	-0.08	2.54	0.12
Platforms (WS>25 m/s)*	26	-0.24	2.60	0.10

* Except K-13

Table 5: Comparison of Wave Model Hindcasts Using NRA & Final QuikSCAT Enhanced Winds vs. Altimeter Wave Measurements 30° - 40° S (2/1/00 – 2/11/01) HS (meters)

	NRA	**NRA QuikSCAT Enhanced**
# of Pts.	92162	92162
Mean Meas.	2.78	2.78
Mean Hind.	2.38	2.63
Mean Diff.	-0.40	-0.15
RMS	0.70	0.57
Std. Dev.	0.58	0.55
Scatter Index	0.21	0.20
Ratio	0.21	0.36
Corr. Coeff.	0.87	0.90

Table 6: Comparison of HS biases (model vs. altimeter) using QuikSCAT corrected wind fields

Location	**# Pts**	**Bias (H-Alt)**	**Scat. Ind.**	**Corr Coeff**
Sea of Okhotsk	12109	-0.08	0.27	0.90
South China Sea	2631	-0.09	0.25	0.89
Irish Sea	676	0.01	0.30	0.84
Offshore Algeria	702	-0.07	0.37	0.86